Vivaspin ultrafiltration: A new approach for high resolution measurements of colloidal and soluble iron species

C. Schlosser[1,2], P. Streu[1], and P. L. Croot[1,3]***Q2**

[1]Helmholz-Zentrum für Ozeanforschung Kiel, GEOMAR, Kiel, Germany
[2]School of Ocean and Earth Sciences, National Oceanography Centre Southampton, University of Southampton, Southampton, United Kingdom
[3]Earth and Ocean Sciences, School of Natural Sciences, National University of Ireland Galway (NUIG), Galway, Ireland

Abstract

Vivaspin6® ultrafiltration units with molecular weight "cut-off" membranes of 5, 10, 30, 50, and 100 kDa were used together to examine the size distribution of newly formed iron (Fe) colloids in natural seawater samples and in the presence of several different Fe chelators with varying Fe binding strength. Artificial Fe chelators, such as TAC, and 2 kDG, when added at equimolar levels to Fe, supported the formation of a continuum of Fe-ligand colloids between 5 and 100 kDa. More than 90% of the added ^{55}Fe in these solutions occurred in Fe aggregates/particles larger than 100 kDa. The strong siderophore DFO held the majority of the added ^{55}Fe in the "truly" soluble fraction ≤ 5 kDa, whereas 90% of ^{55}Fe added to UV-irradiated seawater was converted into Fe colloids with a size between 50 to 100 kDa (5–6 nm). Membranes with ≥ 10 kDa showed similar "cut-off" properties on natural seawater samples collected in the water column off the Peruvian coast. Fe solubility determined with these membranes was approximately six times greater than Fe solubility determined with the 5 kDa membrane and the 0.02 µm syringe filters. This suggests that a seamless size continuum of organic chelators (≤5 kDa–10 kDa) is present in these seawaters and that estimates of ligand production based on 0.02 µm Anotop solubility experiments underestimates the abundance of soluble/colloidal ligands. Regarding these results, we recommend the use of Vivaspin 5 kDa membranes to separate the "truly" soluble from the colloidal Fe fraction.

Most organic and inorganic substances in seawater occur in different size fractions. To investigate these substances separately, different filtration and isolation devices are necessary. Depending on the membrane pore size chosen, filtration can be generally subdivided into macro-, micro-, and ultrafiltration. Macro- (> 50 µm) and microfiltration (0.1–50 µm) are characterized by their membrane pore size in micrometers, whereas ultrafiltration membranes (>0.1 µm) are also defined by their molecular weight "cut-off" (MWCO) in Daltons (Da) (Reitmeyer et al. 1996; Guo et al. 2001; Hassellöv et al. 2007). The molecular weight "cut-off" of ultrafiltration membranes ranges from several thousand Dalton to hundreds and thousands of kilo Dalton (kDa).

Ultrafiltration is thus a powerful technique, which has been used for a wide variety of marine biogeochemical studies, such as investigating the proportion of soluble (≤0.02 µm or ≤ 5 kDa) and colloidal trace metal species (0.02–0.2 µm) within the more routinely measured dissolved size fraction (≤0.2 µm) (Reitmeyer et al. 1996; Boye et al. 2010).

Up to 99% of the dissolved Fe in seawater is complexed by organic chelators (Witter and Luther 1998; Croot and Johansson 2000). These organic chelators (a.k.a. organic ligands) are part of the dissolved organic matter pool (Barbeau et al. 2003; Owen and Butler 2011) and can be formed e.g., through cell lysis (Gobler et al. 1997), zooplankton grazing (Sato et al. 2007), and excretion by bacteria under Fe limitation (Martinez et al. 2000). Iron complexed by these ligands occurs in both the colloidal and soluble size fractions (Boye et al. 2010; Owen and Butler 2011).

Using cross-flow filtration, which is one specific type of ultrafiltration technique (Hassellöv et al. 2007), it has been possible to observe the effect of artificial and natural organic ligands on Fe solubility in seawater. Schlosser and Croot (2008)

showed, by using a 10 kDa membrane for their ultrafiltration set-up, that strong siderophores and organic ligands increase the capacity of seawater for soluble Fe (henceforth in this manuscript referred to as Fe solubility, cFe_s) by one or two orders of magnitude compared to Fe solubility in UV-irradiated Antarctic seawater (~0.15 nmol L^{-1}) (Schlosser and Croot 2008) and artificial seawater (< 0.01 nmol L^{-1}) (Liu and Millero 1999). Schlosser and Croot (2008) also showed that frequently used Fe chelators like ethylenediaminetetraacetic acid (EDTA) and 2-(2-thiazolylazo)-p-cresol (TAC) (used for biological assays and voltammetric experiments, respectively) increase Fe solubility, but also lead to the formation of colloidal Fe (10 kDa–0.2 µm). This occurred when chelators with a weaker Fe binding strength than siderophores were not added in massive excess.

Despite these advances in understanding the Fe cycle, the exact proportion of soluble and colloidal Fe in the dissolved fraction are still unknown due to the limitations of current analytical techniques. In most investigations of Fe solubility and/or soluble and colloidal Fe, only one ultrafiltration membrane has been used, and the exact type was differed between studies (e.g., membrane "cut-off" sizes of 1 kDa [Hassellöv et al. 2007], 3 kDa [Waite et al. 1999], 10kDa [Schlosser and Croot 2008], 200 kDa [Nishioka et al. 2001]). It is very likely that if the organic chelators that control Fe solubility occur across a continuum of sizes, Fe concentrations in the permeate of a 1 kDa membrane will be different to that in the permeate of a 10 kDa (or even larger) membrane. The question arises: "Which 'cut-off' size is needed to truly determine the soluble Fe fraction?" and "In which size continuum does the colloidal Fe fraction appear?"

The problems that arise with interpreting results from Fe solubility experiments where only a single ultrafiltration membrane was used can be avoided by the simple expedient of using several ultrafiltration membranes with different MWCO sizes. This type of approach has been used previously by combining the radiotracer ^{64}Cu with centrifugal ultrafilters with a range of MWCO's 0.5–10 kDa, (Spectrum, Centri/Por) to examine Cu speciation in cultures of the cyanobacterium *Synechococcus* (Croot et al. 2003). For the present study, we employed a series of 6 mL Vivaspin® ultrafiltration units with 5, 10, 30, 50, and 100 kDa membranes. This allowed us to look at differences in the Fe solubility measured in the permeate of the different MWCO membranes, and to determine the fraction of inorganic and organically complexed Fe in the colloidal size range in unamended, natural seawater that contained various different artificial ligands. This is the first study where several different MWCO membranes for ultrafiltration have been simultaneously used for measurements of Fe solubility.

Materials and procedures

Sampling and pretreatment

Bulk surface seawater from the tropical Atlantic (FS *Meteor*, M80-3, Dec 2009–Jan 2010) was collected for artificial Fe ligand solubility experiments using a trace metal clean tow fish deployed over the side of the ship. Seawater was pumped on board through Teflon-coated polyethylene (PE) tubing by a Teflon diaphragm pump (Almatec A-15 TTT). The seawater was passed through a 0.2 µm inline cartridge filter (Sartobran®) into an acid-cleaned 25 L PE carboy and stored otherwise untreated in the dark for several months before use.

During the FS *Meteor* expedition M77-3 that took place between Dec and Jan 2008/09, seawater samples were collected in the upper water column (20–800 m) off the Peruvian coast using trace metal clean Go-Flo bottles. At 6 stations, subsurface seawater samples for dissolved Fe (Fe_D), Fe solubility and CDOM fluorescence measurements were filtered through a 0.2 µm membrane filter (Sartobran). Samples for Fe solubility and CDOM analysis were dispensed into acid-cleaned 125 mL low density polyethylene (LDPE) bottles (Nalgene), stored immediately at –20°C, and shipped frozen to the GEOMAR, Kiel for further analysis. Samples from station Go-Flo 10-11 were further filtered using Vivaspin and 0.02 µm Anotop syringe filters back in the lab. At all stations, CDOM fluorescence was measured.

Filtered seawater samples for Fe_D analysis were dispensed into acid-cleaned 1 L LDPE bottles and immediately acidified with quartz-distilled hydrochloric acid (Q-HCl) to pH 1.75 (~18 mmol $H^+ L^{-1}$), stored in the dark at room temperature, and measured a few months later under clean lab conditions by graphite furnace–atomic absorption spectrometry (GF-AAS) at the GEOMAR in Kiel, Germany. The trace metal analysis method was previously outlined by Danielsson et al. (1978) and Bruland et al. (1979) and described in detail by Grasshoff et al. (1999). The accuracy of the analytical procedure was evaluated by measurement of the certified seawater standard NASS-5 (National Research Council of Canada) and the SAFe intercomparison standard. Our values for NASS 5 agreed within the stated values for NASS 5 and our SAFe data (SAFe S: 0.112 ± 0.013 nmol L^{-1} Fe; SAFe D2: 0.83 ± 0.13 nmol L^{-1} Fe) were close to the average consensus values for Fe (NASS 5: 3.70 ± 0.63 nmol L^{-1}; SAFe S: 0.090 ± 0.007 nmol L^{-1}; SAFe D2: 0.90 ± 0.02 nmol L^{-1}). The precision for replicate analyses was between 3% to 5% at the concentrations found in this study. The procedural (analytical) blank was 0.041 ± 0.024(σ_{bl}) nmol Fe L^{-1}.

Nutrient samples were stored in a –20°C freezer and shipped frozen to the GEOMAR, Kiel and analyzed via an autoanalyzer using the method of Grasshoff et al. (1999). Oxygen concentrations were obtained by an oxygen sensor mounted on a stainless steel CTD. The CTD oxygen data were corrected against oxygen data determined on discrete samples using the Winkler method (Grasshoff et al. 1999).

Ligand solutions

To examine the impact of natural organic chelators on Fe solubility, a broad variety of artificial Fe complexing agents differing in their strength (K_{FeL}, β_2) for complexing Fe were chosen. Organic ligand stock solutions were prepared in deionized water (UV treated Milli-Q water; > 18 MΩ cm^{-1}) (desferrioxamine B [DFO, log K_{FeL} > 13 (Rue and Bruland 1995)]; ethylenedi-

aminetetraacetic acid [EDTA, log K_{FeL} = 7.8 (Hudson et al. 1992)]; and 2-keto-D-gluconic acid [2 kDG, log $_{-2}$ = 11.1 (Essington et al. 2005)]) or in HPLC grade methanol (TAC, log $_{-2}$ = 12.2 [Croot and Johansson 2000]). All organic ligand substances were obtained from Sigma-Aldrich. A small quantity of the ligand stock solutions was added into UV-irradiated surface seawater to give a ligand concentration of 100 nmol L^{-1}. Natural seawater from M80-3 was irradiated for 75 min in 10 mL acid-cleaned quartz glass vials in a Metrohm 705 UV Digester. The seawater-ligand solutions, however, were allowed to equilibrate for at least 24 h following the addition of ^{55}Fe.

Sample treatment: Fe solubility

Fe solubility measurements were performed using the radioisotope ^{55}Fe (Hartmann Analytics). The ^{55}Fe solution had a specific activity of 96.23 MBq mg^{-1} Fe, a total activity of 74 MBq, and was dissolved in 0.1 mol L^{-1} HCl. Further dilutions were prepared using deionized water and were acidified with Q-HCl. The experimental setup for the measurement of Fe solubility by 47 membrane filtration (Millipore MF) was adapted from Kuma et al. (1996) and Nakabayashi et al. (2002). For examining the artificial ligand solutions, 100 nmol L^{-1} of ^{55}Fe was added at t_0 into each artificial ligand-seawater solution (L = 100 nmol L^{-1}), whereas 20 nmol L^{-1} of ^{55}Fe was added into the 0.2 µm filtered natural seawater samples collected during M77-3. As noted earlier, these natural seawater samples were stored frozen and thawed just shortly before the ^{55}Fe treatment.

Anotop syringe filtration

After the addition of ^{55}Fe, and an equilibration time of 72 h, 10 mL of each sample was filtered through a 0.02 µm Anotop syringe filter (Whatman®) that had been first flushed and then filled with MQ water. The first 7.5 mL of the 10 mL filtrate was rejected to avoid dead volume artifacts. The remaining seawater, 1 to 2 mL, was directly injected into a small, acid-cleaned Teflon bottle and acidified with 20 µL of Q-HCl to a pH below 1.8. A small volume (400 µL) of filtered sample was transferred into duplicate 6 mL scintillation counting vials to which 4.5 mL counting cocktail (Lumagel Plus®) were added.

After filtration and counting cocktail addition, the closed vials were placed in a liquid scintillation counter (Packard, Tri-Carb 2900TR) and counted for at least 30 min. Throughout all this, the samples were handled at room temperature (~20°C) and stored in the dark.

Vivaspin6 filtration

5 mL of each seawater solution was transferred into the 100 kDa, 50 kDa, 30 kDa, 10 kDa, and 5 kDa Vivaspin6 filter reservoirs that had been rinsed with MQ by centrifugation for 5 min. The Vivaspin6 filters were then placed in an unheated centrifuge (Eppendorf Centrifuge 5430 R) for 10 min at ~5000 rpm (1300 g). The permeate was acidified with 20 µL Q-HCl to avoid any wall sorption artifacts. In duplicate, 400 µL of the remaining retentate and 400 µL of the filtered permeate were transferred each into 6 mL scintillation counting vials to which 4.5 mL of the counting cocktail were added. The same

counting procedure as used for the Anotop syringe samples was applied to the Vivaspin6 samples.

After each filtration, the ultrafiltration housings and membranes were cleaned with a diluted Q-HCl solution and MQ. 5 mL of a 0.05 M Q-HCl solution were transferred into the used ultrafiltration unit, which then was spun in the centrifuge for at least 10 min. 400 µL of the permeate was transferred into a 6 mL counting vial to which 4.5 mL counting cocktail were added. The activity of ^{55}Fe in the Q-HCl wash solution was then used for mass balance calculations.

All Vivaspin and Anotop filtrations were performed in duplicate (n = 2). The Fe concentration that passed the 0.02 µm Anotop filters and the Vivaspin6 membranes are the values reported in this manuscript for Fe solubility at 0.02 µm (0.02 µm cFe$_S$), 'truly' soluble Fe at 5 kDa (5 kDa cFe$_S$), Fe solubility at 10 kDa (10 kDa cFe$_S$), Fe solubility at 30 kDa (30 kDa cFe$_S$), Fe solubility at 50 kDa (50 kDa cFe$_S$), and Fe solubility at 100 kDa (100 kDa cFe$_S$).

CDOM measurements

Subsamples from the thawed samples (M77-3) were immediately measured for their colored dissolved organic matter (CDOM) fluorescence using a Hitachi F-2700 FL Spectrophotometer with a 1 cm quartz glass cuvette. The analytical protocol for single excitation-emission CDOM$_{320/420}$ measurements was adapted from Hayase et al. (1988) **Q3** and Hayase and Shinozuka**Q4** (1995). The intensity of fluorescence was expressed in terms of quinine sulfate content (1 QSU = 1 ppb quinine in 0.05 mol H_2SO_4 at 320 nm excitation and 420 nm emission), corrected for the MQ blank, and then converted into the unified scale of Raman units (Lawaetz and Stedmon 2009).

In addition to single wave length excitation-emission measurements, excitation-emission matrices (EEM) (Yamashita et al. 2010) were generated for all samples. The instrumental protocol was followed for this approach. The EEM matrixes were generated by scanning fluorescence emissions between 240–800 nm caused by excitation between 220–600 nm in steps of 10 nm wavelength. Sample fluorescence was normalized to daily measurements of the fluorescence of quinine standards (QSU) (Mopper and Schultz 1993) or to the Raman-induced fluorescence of water (excitation 350 nm) (Stedmon et al. 2003). The normalized EEMs were analyzed by PARAFAC in MATLAB using the DOMFluor toolbox (Stedmon and Bro 2008). In this work, using split half analysis, three components were validated. No samples were removed from the dataset.

Assessment

Artificial ligand solutions

With the exception of DFO, all artificial ligand-seawater solutions showed similar Fe solubilities of ~ 5 nmol L^{-1} (Table 1) when filtered through the 100 kDa membrane. This roughly corresponded to 1/20 of the initial Fe concentration (100 nmol L^{-1}). Fe solubility decreased stepwise when these ligand-seawater solutions were filtered through the 50 kDa, 30

Table 1. The table shows ^{55}Fe concentration at time zero ($t_0 \sim 100$ nmol L^{-1}) and after 72 h (t_t) for syringe filtration and permeate (perm. in nmol L^{-1}) and retentate (ret. in nmol L^{-1}) associated with ultrafiltration, and the mass balance (in percent) for the various artificial organic chelators and ultrafiltration membranes used. The syringe filtration technique used did not allow the determination of the concentration of the retentate.

	Fe-(DFO) perm./ret. (m.b.) (nmol L^{-1}/nmol L^{-1} (%))	Fe-(EDTA) perm./ret. (m.b.) (nmol L^{-1}/nmol L^{-1} (%))	Fe-(TAC) perm./ret. (m.b.) (nmol L^{-1}/nmol L^{-1} (%))	Fe-(2kDG) perm./ret. (m.b.) (nmol L^{-1}/nmol L^{-1} (%))	Fe-SW perm./ret. (m.b.) (nmol L^{-1}/nmol L^{-1} (%))	Fe-UVSW perm./ret. (m.b.) (nmol L^{-1}/nmol L^{-1} (%))
t_0/t_t	102.95/93.33	94.85/90.56	98.93/85.16	96.72/81.98	99.81/93.27	95.64/85.40
0.02 µm	80.85	4.77	2.65	1.95	1.56	0.91
5 kDa	81.94/106.29 (98.88)	5.58/87.09 (95.69)	1.76/77.03 (100.09)	2.10/52.73 (91.50)	2.27/85.67 (93.44)	1.87/68.41 (86.04)
10 kDa	80.15/102.90 (96.95)	6.79/75.67 (88.80)	3.38/68.60 (89.92)	3.73/76.61 (92.90)	4.43/75.33 (101.37)	3.26/64.12 (91.03)
30 kDa	80.68/101.70 (97.44)	6.50/— (—)	3.55/73.96 (88.96)	3.36/62.33 (89.72)	3.87/79.40 (99.38)	2.74/111.38 (107.46)
50 kDa	82.37/99.38 (99.03)	6.75/74.83 (88.07)	4.13/83.40 (91.08)	3.68/63.41 (85.59)	4.92/76.43 (95.83)	4.91/42.50 (99.75)
100 kDa	81.35/100.92 (100.18)	6.61/87.65 (87.25)	4.48/93.58 (94.80)	4.03/127.59 (90.13)	5.11/123.09 (13.94!)	90.85/39.26 (89.48)

kDa, 10 kDa, and 5 kDa membranes (Table 1, Fig. 1). The largest difference in cFe_S between the 100 kDa and 5 kDa membrane was found for the TAC seawater solution (ΔcFe_S = 2.72 nmol L^{-1}). The smallest difference was observed for the EDTA seawater solution (ΔcFe_S = 1.03 nmol L^{-1}). An intermediate decrease was determined for the 2 kDG seawater mixture (ΔcFe_S = 1.93 nmol L^{-1}). DFO, a strong siderophore produced by terrestrial bacteria, showed nearly the same Fe solubility value of 81 ± 1 nmol L^{-1} (σ, n = 2) over the whole range of ultrafiltration membranes and also with the 0.02 µm Anotop syringe filtration. All other ligand-seawater solutions generally showed a reduction in Fe solubility when filtered through the 0.02 µm Anotop syringe filter (Table 1).

When natural untreated seawater (no UV oxidation, no ligand addition) sampled directly from the 20 L storage tank was used, the difference between the Fe solubility assessed with the 100 kDa cutoff and the "true" Fe solubility at 5 kDa and with the 0.02 µm syringe filtration was similar to the results obtained with the artificial ligand-seawater experiments (Fig. 1). However, this was not the case when ^{55}Fe was added after the same seawater had been irradiated with UV for at least 75 min. Nearly 91% of the initially added ^{55}Fe was able the pass the 100 kDa membrane. This amount decreased to 4.91 nmol L^{-1} using the 50 kDa filter, and to 1.87 nmol L^{-1} when the UV-treated seawater was passed through the 5 kDa filter. The amount of soluble Fe that was able to pass the 0.02 µm Anotop filter (0.91 nmol L^{-1}) was approximately half the "truly" soluble Fe concentration that passed the 5 kDa membrane filter but still six times greater than previously outlined results for UV-irradiated seawater by Schlosser and Croot (2008).

Between 85% and 100% of the initially added ^{55}Fe could be recovered from the used Vivaspin polycarbonate filter housing and the polyethersulfone (PES) membrane using a brief acid and MQ rinse, as outlined in the method section (Table 1). This suggests that both the Vivaspin6 and the Vivaflow 50® filters (Schlosser and Croot 2008) can be re-used several times when sufficient acid cleaning and MQ rinse is carried out between filtrations.

Fe solubility depth profile off the Peruvian coast

The same filtration procedure as described for the artificial ligand-seawater solutions (Vivaspin and 0.02 µm syringe filtration) was conducted on natural seawater samples collected in the water column off the Peruvian coast (Fig. 2) but adding only just 20 nmol ^{55}Fe L^{-1} to each natural seawater sample.

Highest Fe solubilities were determined after 72 h (2.09–6.04 nmol L^{-1}) when the seawater samples were filtered through ultrafiltration membranes ≥ 10 kDa (Fig. 3, Table 2), with just minor differences seen for samples filtered through the 100, 50, 30, and 10 kDa ultrafiltration membranes. Fe solubilities were remarkably lower when samples were filtered through the 5 kDa membranes ("true" Fe solubility ~ 0.70–1.05 nmol L^{-1}), or through the 0.02 µm Anotop filter (0.52–0.72 nmol L^{-1}). However, the depth profiles look simi-
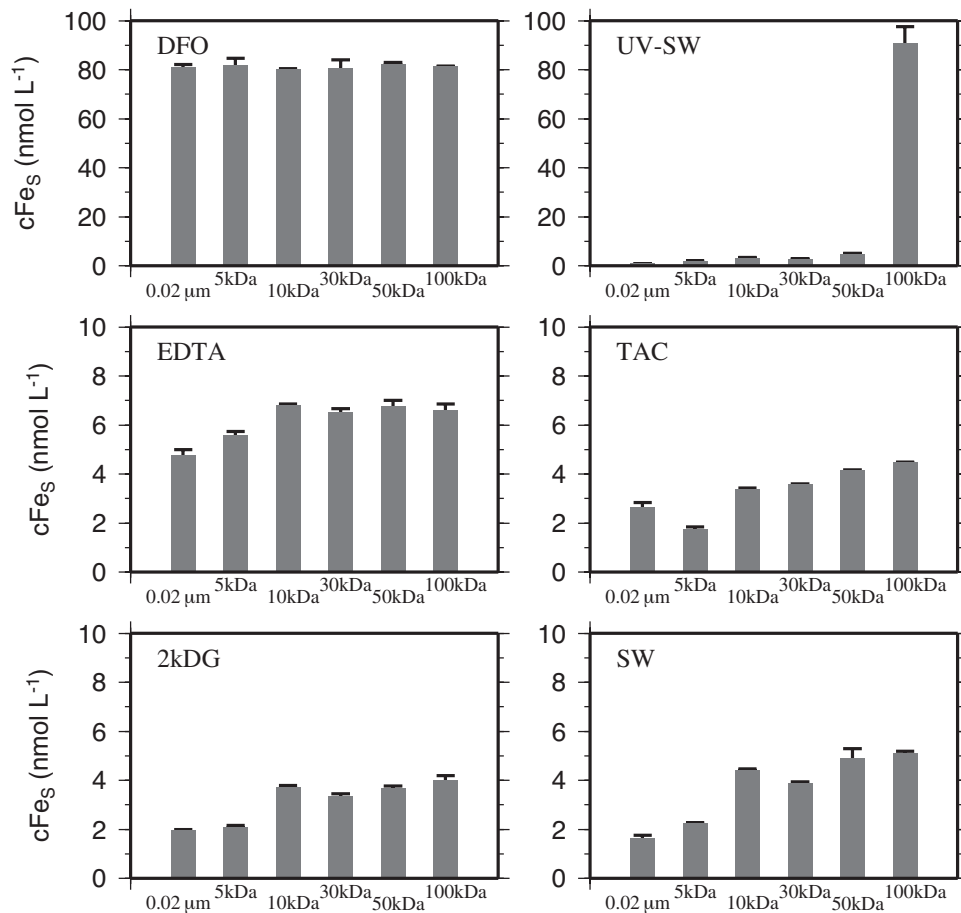
Fig. 1. Fe solubility of DFO, TAC, EDTA, 2kDG, UV-irradiated, and untreated tropical Atlantic seawater solutions filtered in duplicates through a 0.02 μm Anotop syringe filter and through 5, 10, 30, 50, and 100 kDa ultrafiltration Vivaspin membranes. Please note the different Fe solubility scaling used for DFO and UV-irradiated seawater solutions. Errors shown correspond to the total uncertainty associated with pipetting, decay counting, and filtration (*n* = 2).
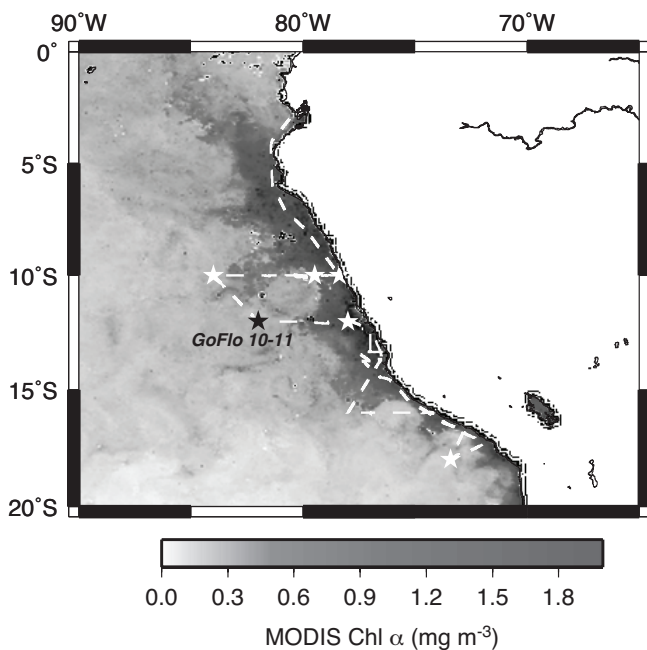

Fig. 2. (Left) Locations where seawater samples were collected off the Peruvian coast during FS *Meteor* M77-3 in Dec 2008–Jan 2009 (white and black stars). Of special interest for this study were the samples collected from station Go-Flo 10-11 (black star at 12°S and 82°W). The cruise track of M77-3 is shown by the dashed white line and the chlorophyll α (Chl α) concentration recorded by the MODIS satellite is shown by the shades of gray. Close to the shore, Chl α concentrations reached values of up to 30 mg m^{-3} (black areas).

lar (Fig. 3), even though the actual Fe solubilities determined from the 5 kDa and 0.02 μm syringe filtration were approximately one-sixth of those determined from membranes ≥ 10 kDa. Despite the differences in absolute values of solubility, data obtained from all filtration devices showed a surface minimum (≥10 kDa: 2.65–3.65 nmol L^{-1}), a strong subsurface maximum between 150 m and 200 m (≥10 kDa: 4.97–6.04 nmol L^{-1}) that was significantly more strongly developed for MWCO ≥ 10 kDa, and almost constant values (≥10 kDa: 2.09–3.59 nmol L^{-1}) for Fe solubility at depths between 400 and 800 m.
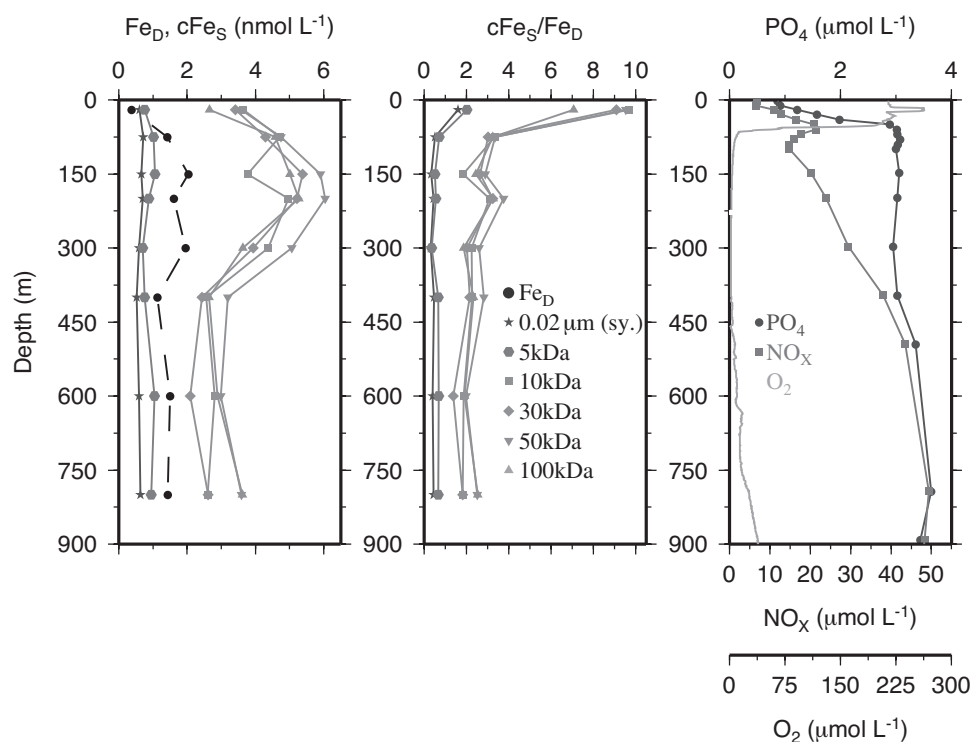
Fig. 3. (Left panel) Dissolved Fe concentrations (dashed black line) and Fe solubility determined using Vivaspin6 ultrafiltration membranes and 0.02 μm Anotop syringe filtration on samples collected at Go-Flo station 10-11. 20 nmol L^{-1} of ^{55}Fe was added to the 0.2 μm filtered seawater samples to determine Fe solubility. (Middle panel) Ratios of cFe$_S$/Fe$_D$ in the water column and the legend for the left and middle panels are shown here. (Right panel) Phosphate (black), nitrite + nitrate (dark gray), and oxygen concentrations (bright gray) are shown for station Go-Flo 10-11.

Discussion

Ultrafiltration is a common way to separate and identify soluble Fe species and characterize artificial and natural chelators for their ability to complex Fe, and in this way, increase Fe solubility. Fe chelators tested in this work have been recently characterized in detail via cross-flow filtration with a 10 kDa membrane (Schlosser and Croot 2008), allowing a short introduction to each substance to be given below.

Desferrioxamine B is a strong hydroxamate siderophore (Schwarzenbach and Schwarzenbach 1963) that is produced by terrestrial bacteria and forms strong Fe complexes (K$_{FeL}$ > 13 [Rue and Bruland 1995], K$_{Fe'L}$ > 16 [Croot and Johansson 2000]) under ambient seawater conditions (Hudson et al. 1992). Assuming an inorganic Fe solubility of 0.15 nmol L^{-1} (Schlosser and Croot 2008) or 0.01 nmol L^{-1} (Liu and Millero 1999) and that all organically complexed Fe species are "truly" soluble (<5 kDa) the amount of soluble Fe ([*Fe(III)L*] + [*Fe(III)′*]) can be estimated by: K$_{FeL}$ = ([*Fe(III)L*] / [*Fe(III)′*][*L′*]) = 10^{13}. For DFO this yields a soluble Fe fraction of ~ 100 nmol L^{-1}. Experiments have shown that DFO is a very strong Fe complexing agent (Cheah et al. 2003; Cheah et al. 2006; Kim et al. 2010), and consequently DFO has been used extensively to limit Fe availability to phytoplankton in incubation experiments (Hutchins et al. 1999). At a 1:1 ratio between ligand and ^{55}Fe,

slightly more than 80% of the ^{55}Fe was organically complexed by DFO and passed equally through all ultrafiltration membranes and the 0.02 μm Anotop syringe filter. The remaining 20% of the initially added ^{55}Fe was retained by the different filtration devices, but were easily remobilized when the housing and PES membrane filter was rinsed with a 0.05 mol L^{-1} Q-HCl solution. Regarding the fact that the ^{55}Fe concentration within the LDPE reservoir decreased by 10 nmol L^{-1} after 72 h (due to wall sorption [Schlosser et al. 2011]), the remaining10% must have been lost to scavenging onto surfaces of the Vivaspin PC housing and/or the PES filter. This was also true for the other ligand-seawater solutions.

Fe-EDTA complexes are also well described in the literature (Gerringa et al. 2000; Sunda and Huntsman 2003) and indicate that this substance forms three relatively weak Fe complexes, Fe(OH)(EDTA)$^{2-}$, Fe(OH)$_2$(EDTA)$^{3-}$, and Fe(EDTA)$^{-}$ (K$_{Fe(III)'L}$ = 10$^{7.8}$). Solubility calculations as performed for DFO yield Fe solubility ([*Fe(III)L*] + [*Fe(III)′*]) values of 1.1 nmol L^{-1} and 0.07 nmol L^{-1}, for 0.15 nmol L^{-1} and 0.01 nmol L^{-1} inorganic Fe solubility, respectively. However, a small fraction of the added ^{55}Fe (~ 5 nmol L^{-1}) in the EDTA treatment was able to pass through 5 kDa membrane, which is just slightly less than what passed through the ultrafiltration membrane with the largest "cut-off" size of 100 kDa (<7 nmol L^{-1}). The measured Fe-EDTA solubility values determined in this work and

Table 2. The table shows dissolved Fe concentration (Fe$_D$), Fe solubility (20 nmol L^{-1} of ^{55}Fe were added to 0.2 µm filtered seawater samples) for the different filtration devices used, and the amount of dissolved oxygen (O$_2$) measured in water samples collected offshore the Peruvian coast (Go-Flo 10-11; at 12° and 82°W; 5 Jan 09**Q5** at 19:45 GMT). The table shows also the CDOM$_{320/420}$ fluorescence in Raman units, and the amount of Humic1, Humic2, and Protein1 computed by the PARAFAC algorithm (EEM data, Table S1).

Depth (m)	Fe$_D$ (nmol L^{-1})	0.02 cFe$_s$ (nmol L^{-1})	5 kDa cFe$_s$ (nmol L^{-1})	10 kDa cFe$_s$ (nmol L^{-1})	30 kDa cFe$_s$ (nmol L^{-1})	50 kDa cFe$_s$ (nmol L^{-1})	100 kDa cFe$_s$ (nmol L^{-1})	O$_2$ (µmol kg^{-1})	CDOM$_{320/420}$ (R.U.)	Humic1 (R.U.)	Humic2 (R.U.)	Protein1 (R.U.)
20	0.38	0.61	0.76	3.65	3.42	3.58	2.65	261.9	0.081	0.016	0.015	0.032
75	1.42	0.72	1.01	4.71	4.29	4.75	4.57	9.1	0.119	0.019	0.017	0.019
150	2.04	0.67	1.05	3.77	5.38	5.91	5.00	3.6	0.098	0.017	0.015	0.014
200	1.61	0.70	0.88	4.97	5.21	6.04	5.27	2.5	0.122	0.018	0.015	0.013
300	1.95	0.59	0.70	4.38	3.94	5.07	3.63	1.9	0.102	0.018	0.013	0.013
400	1.13	0.52	0.76	2.56	2.44	3.19	2.64	2.3	—			
600	1.50	0.60	1.04	2.80	2.09	2.98	2.89	10.3	—			
800	1.43	0.63	0.95	2.61	2.62	3.59	3.62	26.6	—			

in the study of Schlosser and Croot (2008) exceed the calculated values. The reason for this is not clear. The results indicate that EDTA and Fe, when added to seawater in a 1:1 molar ratio, form very few soluble Fe complexes compared to DFO.

TAC is frequently used for voltammetric Fe speciation measurements (Croot and Johansson 2000) and belongs to the family of thiazolylazo compounds (Hovind 1975), forms strong Fe complexes (Fe(TAC)$_2$), and when employed in excess, tends to increase the soluble Fe fraction ($_{Fe'(TAC)2}$ = $10^{12.4}$). Our ultrafiltration and syringe filtration experiments showed that in the presence of TAC very little (<5 nmol L^{-1}) of the initially added ^{55}Fe (100 nmol L^{-1}) was able to pass through the membranes and the syringe filter. This suggests that adding TAC and Fe into seawater in a 1:1 molar ratio does not lead to appreciable concentrations of Fe within the soluble size fraction (≤5 kDa).

The chelator 2 kDG is a natural product of glucose oxidation. It has been suggested that 2 kDG is an important chelator for trace metals in soils (Nelson and Essington 2005) and related compounds may play an important role in the photoreduction of Fe in seawater (Öztürk et al. 2004) ($\beta_{Fe(OH)3(2kDG)2}$ = $10^{11.1}$). However, our results suggest that 2 kDG at a 1:1 molar ratio with Fe only produces a small amount of organic Fe complexes in the soluble size fraction (~4 nmol L^{-1}).

Comparison of Vivaspin6 with Vivaflow50 experiments (both 10 kDa)

Although the Vivaspin6 (tested here [Table 1]) and Vivaflow50 (tested in Schlosser and Croot [2008]) filters both had an apparent MWCO of 10 kDa, different amounts of ^{55}Fe in the EDTA and in the TAC-seawater solution passed through the different membranes. Lower concentrations of ^{55}Fe passed through the 10 kDa Vivaspin6 membrane (6.79 nmol L^{-1} for EDTA and 3.38 nmol L^{-1} for TAC) than through the Vivaflow50 10 kDa membrane (15 nmol L^{-1} for EDTA and 6 nmol L^{-1} for TAC). The observed deviation is most likely related to the difference in the volume to surface ratio and flow rates between the two filter setups. The Vivaflow50 10 kDa membranes employed by Schlosser and Croot (2008) have a surface area of ~ 50 cm^2, approximately 20 times greater than the surface area of the Vivaspin6 membranes (2.5 cm^2) that are built into centrifuge tubes. Membrane blocking of the smaller Vivaspin6 filters by the artificial ligands that were added and by remnants of natural dissolved organic matter in the UV-irradiated seawater cannot be ruled out, although it would be surprising if the amount of organic matter remaining after 75 min UV treatment or added as artificial ligands (100 nmol L^{-1}) was able to block the membranes.

The situation is reversed for solubilities determined for the UV-irradiated seawater and seawater containing DFO or 2kDG. Fe solubility in the DFO-seawater solution were roughly twice as large when filtered through the Vivaspin6 10 kDa membrane (80 nmol L^{-1}) than when filtered through the Vivaflow 50 10 kDa membrane (47 nmol L^{-1} (Schlosser and Croot 2008)). The same was found for the 2 kDG-seawater solution

(3.73 nmol L^{-1} versus 1.15 nmol L^{-1}), and for the UV-irradiated seawater (1.87 nmol L^{-1} versus 0.15 nmol L^{-1}).

Both the Vivaspin6 10 kDa membrane and the Vivaflow50 10 kDa membrane are made of the identical polyethersulfone (PES) material. Both membranes should thus have the same physical and chemical properties and should behave similarly in terms of the retention and permeation of truly dissolved and colloidal materials that are suspended in seawater. However, the results of ultrafiltration experiments differ greatly from earlier measurements made by Schlosser and Croot (2008). It is not clear what causes the differences between the filtration techniques. We suggest that the most likely explanation is the difference in the volume to surface area between the filters and/or a thermal effect from the centrifugation even though when just performed for a short time (~10 min.).

Size continuum of artificial Fe chelators and inorganic Fe

Natural ligands increase the solubility and residence time of Fe in seawater (Rue and Bruland 1997). This implies that "truly" soluble Fe complexing agents in excess with respect to artificially added Fe should permit the majority of the ^{55}Fe to pass through the 5 kDa filter membrane. Regarding the slight but steady increase of ^{55}Fe able to pass through the ultrafiltration membranes with increasing "cut-off" size, the Vivaspin6 filtration experiments showed that artificial Fe complexes, like Fe-EDTA, Fe-TAC, and Fe-2kDG occur in a size continuum of colloids between 5 kDa to 100 kDa (Table 1 and Fig. 1). However, the retention of the majority of the added ^{55}Fe (more than 90%) in these ligand-seawater solutions, even when the largest 100 kDa Vivaspin6 membrane was used, suggests that even larger Fe-ligand colloids or particles ≥ 100 kDa were formed.

By subtracting the amount of "truly" soluble ^{55}Fe that passed the 5 kDa membrane from the amount of ^{55}Fe that passed the 10 kDa membrane, the amount of colloidal ^{55}Fe contained within the weight range between 5 and 10 kDa was calculated (Table 3). The same were done for the other MWCO membranes (Table 3). These calculations yield a size distribution of the different colloidal organically complexed ^{55}Fe species between < 5 kDa, 5 kDa and 10 kDa, 10 kDa and 30 kDa, 30 kDa and 50 kDa, 50 kDa and 100 kDa, ≥ 100 kDa. Iron in Fe-EDTA, Fe-TAC, and Fe-2kDG solutions, and in natural untreated seawater, appeared mostly (~94%) as large col-

loids/particles ≥ 100 kDa, although a small fraction of smaller colloids were also formed in the ranges 5–10 kDa (~ 1.7%), 30–50 kDa (0.1%), and 50–100 kDa (0.3%). Only a small fraction (2–6%) of Fe in these solutions remained in the "truly" soluble range < 5 kDa (Table 3). In contrast, most of the Fe in the Fe-DFO solution (~80%) passed with equal efficiency through all of the ultrafiltration membranes used. These findings support the idea that Fe-DFO complexes do not tend to form large colloids and instead occur mostly as smaller MW compounds in seawater (MW = 803, Batinic-Haberle et al. 1994; Iwade et al. 2006).

Most interesting were the Fe solubility results for the UV-irradiated seawater. It is well accepted that strong UV radiation removes somewhere between the majority and the entirety of dissolved organic matter (DOM) in seawater (Achterberg et al. 2001; Ndung'u et al. 2003), allowing the behavior of inorganic Fe species in DOM-free seawater to be examined. In this case, just a small fraction of ^{55}Fe was found in the "truly" soluble size fractions ≤ 5 kDa (1.96%) or in the colloidal fractions between 5–10 kDa (1.46%), 10–30 kDa (0%), and 30–50 kDa (2.27%). However, up to 90% of the ^{55}Fe added into UV-irradiated seawater passed through the 100 kDa membrane, suggesting that after 72 h colloidal inorganic Fe existed mostly between 50 and 100 kDa in size. This finding supports results of earlier studies, which examined the rapid formation of Fe colloids (Nowostawska et al. 2008) that were unable to pass through Millipore FM filters (25 nm) (Hove et al. 2007; Croot et al. 2011).

Iron added to UV-irradiated seawater in the form of acidified Fe standard solutions undergoes rapid changes (Schlosser et al. 2011). The strong shift in pH from that of the Fe standard solution (~pH 1) to that of seawater (~pH 8) causes soluble Fe to be quickly transformed into Fe(III) oxyhydroxide colloids. Freshly precipitated Fe(III) oxyhydroxides are very fine colloids and particles with large surface area and structural disorder. They have a very low thermodynamic stability and a high Fe(III) solubility. These Fe(III) oxyhydroxides easily undergo chemical changes with time (loss of water and increased crystallization). These chemical changes are strongly dependent on the water temperature, with lower values for Fe(III) solubility associated with higher temperatures and longer aging times (Kuma and Matsunaga 1995; Kuma et al.

Table 3. Table shows the size fractions of artificial FeL and inorganic Fe size in percentage. The last row (>100 kDa) illustrates the missing percentage of ^{55}Fe that was retained by the 100 kDa membrane.

Vivaspin6 (kDa)	^{55}Fe-DFO (%)	^{55}Fe-EDTA (%)	^{55}Fe-TAC (%)	^{55}Fe-2 kDG (%)	Inorg. ^{55}Fe (%)
≤5	87.79	6.16	2.07	2.56	1.96
5–10	0.00	1.34	1.90	1.99	1.46
10–30	0.56	0.00	0.20	0.00	0.00
30–50	1.82	0.28	0.68	0.39	2.27
50–100	0.00	0.00	0.41	0.42	89.85
> 100	9.83	92.22	94.73	94.64	4.46

1996; Iwade et al. 2006; Yoshida et al. 2006). The inorganic Fe colloid sizes found (50–100 kDa) must be therefore understood as a snapshot of Fe colloid sizes after 72 hours.

The weight unit (Dalton) is not a SI unit and cannot be converted into dimensions of length (e.g., nm). However, making the following assumptions, an approximate size in nanometer for inorganic Fe colloids can be computed. One Dalton corresponds to the mass of 1/12 of the carbon isotope ^{12}C, which is equal to one atomic mass unit (1 u) or $\approx 1.66 \times 10^{-27}$ kg. The maximum weight of a simplified spherical molecule this could pass a 5000 Da membrane is then 8.30×10^{-21} g. That corresponds to the mass of 416 carbon atoms ^{12}C (or 56 atoms of ^{55}Fe) and is equal to a simplified sphere volume of 2.20 nm^3, when an atomic radius of 0.108 pm for the carbon atoms was applied (210 pm for Fe). The diameter of the sphere volume can then be easily calculated. Assuming that the cubic close packing filled 74% of the total sphere volume, 5 kDa (the "truly" soluble cutoff) corresponds to a pore size of 2.18 nm. This suggests that the inorganic Fe colloids that did not pass 50 kDa membrane, but passed the 100 kDa membrane, had an effective diameter between 4.70 nm and 5.92 nm.

A colloid with the size of ~ 5 nm should have easily passed the 0.02 µm Anotop syringe filter membrane. This was obviously not the case (Fig. 1). However, the Fe solubility determined with the 0.02 µm syringe filters corresponded roughly with the permeability of the "truly" soluble "cut-off" 5 kDa membrane filters. In accordance with the earlier described pore size calculations, 5 kDa membranes should have a pore size of ~ 2 nm. Chen et al. (2004) reported that Anotop filters were considerably different from their rated pore size of 0.02 µm. Using fluorescein-tagged macromolecular compounds, they noted that the Anotop filters had an actual "cut-off" of ~ 3 kDa. Our results agree with the findings of Chen et al. (2004). This discrepancy, however, is troubling given the frequency with which these 0.02 µm aluminum oxide filters from Whatman® have been used and interpreted as having a larger MWCO.

Size continuum of natural Fe chelators in natural seawater

Natural seawater samples were collected up to 300 nautical miles offshore from the Peruvian coast in the latitudinal core of the tropical East Pacific oxygen minimum zone (Fig. 2). This part of the ocean is influenced by strong upwelling and is characterized by elevated primary production in the euphotic and oxygen-containing zone (Fig. 2). Below the mixed layer (10–25 m) oxygen (O_2) was depleted down to hypoxic and anoxic conditions and macronutrient concentrations (phosphate [PO_4], nitrite + nitrate [NO_x]) were elevated (Fig. 3, Table 2). These oxygen-depleted zones are the result of elevated bacterial degradation of organic matter, which consumed the majority of dissolved oxygen and strong vertical stratification reduced the ventilation of the deeper waters.

The O_2 content of seawater plays a key role in the speciation of Fe and other redox sensitive metals. Under hypoxic and anoxic conditions, for instance, Fe(III) can be quickly reduced to the more soluble and more bioavailable Fe(II) species (Hong and Kester 1986). This would result in overall enhanced dissolved Fe concentrations and probably also higher soluble iron concentrations in oxygen minimum zone waters (Lohan and Bruland 2008). In agreement with previously published data from Hong and Kester (1986), we determined elevated dissolved Fe concentrations (Fe_D: ~ 2 nmol L^{-1}) in the low oxygen containing waters between 70 m and 400 m depth (Fig. 3). Unpublished Fe(II) data from the same station (pers. comm. A. Dammshaeuser, GEOMAR and P. L. Croot) suggest that these elevated dissolved Fe concentrations were most likely related to high concentrations of the reduced iron species Fe(II).

As pointed out in the introduction, dissolved Fe in oxygenated seawater consists of a soluble and colloidal fraction (Wu et al. 2001; Boye et al. 2010), where 99% of the dissolved Fe is complexed by soluble and colloidal organic chelators (Boye et al. 2010). Assuming that differences in water temperature and oxygen content were eliminated by sampling and sample storage (bottle head space, etc) differences in Fe solubility in the water samples were strictly related to the amount of organic chelators present in the samples.

Natural and artificially added ^{55}Fe in the seawater samples are in equilibrium after 72 hours (Schlosser et al. 2011). Due to this, the amount of soluble and colloidal Fe in the dissolved Fe fraction can be calculated by subtracting the "true" Fe solubility determined using the 5 kDa membranes from the dissolved Fe concentration. The "true" Fe solubility exceeded the dissolved Fe concentration at 20 m water depth (Fig. 3). Assuming an inorganic Fe solubility of 0.15 nmol L^{-1} (Schlosser and Croot 2008) "truly" soluble natural ligands were in excess (~0.16 nmol L^{-1}) with respect to dissolved Fe. Because Fe_D concentrations exceeded the "true" Fe solubility in samples from below the surface layer, the dissolved Fe pool consisted of both a soluble and colloidal fraction. Above 75 m and below 400 m, outside the anoxic core zone, soluble Fe accounts for ~45% of the dissolved Fe pool. Although the overall concentration of the soluble Fe pool slightly increased in the anoxic core region between 75 m and 400 m, soluble Fe was a smaller proportion of the dissolved Fe pool (~33%). Results of colloidal Fe measurements published by Boye et al. (2010) were slightly lower (colloidal Fe: 37–51%) than the contribution of colloidal Fe in the dissolved Fe pool determined for this study (colloidal Fe 50–75%). Both studies showed that more soluble Fe contributes to the dissolved Fe pool in the surface layer. However, our approach did not consider that inorganic Fe solubility might change greatly under anoxic conditions due to the contribution of more soluble Fe(II) species. Due to this, our approach probably overestimates the amount of colloidal organic Fe in the anoxic core region of the oxygen minimum zone.

Vivaspin membranes ≥ 10 kDa showed generally higher Fe solubilities throughout the water column (≥ 2 nmol L^{-1}) (Fig. 3). As already shown for the 5 kDa membranes, highest solu-

bilities for Vivaspin membranes ≥ 10 kDa were achieved in samples from the core region of the oxygen minimum zone (~6 nmol L^{-1}). This finding was quite unexpected, since Fe_D concentration from this particular depths were already elevated (1.1–2.0 nmol L^{-1}). It seems that natural organic Fe chelators in different sizes clusters (≤5 kDa ["truly" soluble] and 5–10 kDa [colloidal]) or in a seamless size continuum between ≤5 kDa–10 kDa were responsible for elevated Fe solubilities found for water samples collected in the core of the oxygen minimum zone. This does not rule out the presence of inorganic Fe colloids. However, it is likely that the continuous but slow aging process of inorganic colloids, converting them from $Fe(OH)_3$ to amorphous FeOOH, was sufficiently affected by the presence of DOM and organic ligands (Liu and Millero 2002) in the seawater samples.

Organic Fe chelators are released in various ways; one is through the bacterial decomposition of organic matter, where macronutrients and organic chelators are excreted simultaneously. Supporting this is the linear relationship of apparent oxygen use (AOU), phosphate concentration, and pH (release of CO_2) with Fe solubility shown by Schlosser and Croot (2009) and Tani et al. (2003). However, a linear dependence between Fe solubility and phosphate concentrations was not observed for the samples in this study (Fig. 3). The lack of relationship between Fe solubility and phosphate may be due to the strong phosphate gradient and that only one sample was collected in the uppermost 70 m of the water column for the measurement of cFe_S.

Concentrations of Fe-binding ligands in seawater vary from region to region. Coastal seawater has significantly higher ligand concentrations (7 to 70 nmol L^{-1}, Croot and Johansson 2000) than open ocean seawaters (0.5 to 6 nmol L^{-1}, Powell and Donat 2001; Croot et al. 2004a; Croot et al. 2004b), related to its overall higher biological activity. The 0.02 µm Anotop syringe filtration experiments and voltammetric ligand measurements in the past, led to the conclusion that just a small amount of organic ligands were present in the soluble size fraction (Schlosser and Croot 2009). Stolpe and Hassellhov (2010) used flow field fraction (FFF) for their colloidal research (1 kDa–0.45 µm) in seawater samples and showed that colloidal organic Fe mostly exists in sizes between 0.5–3 nm and 7–40 nm. However, it appears that the colloidal ligand pool within the dissolved fraction is partly captured when the 10 kDa Vivaspin ultrafiltration membranes are used for ^{55}Fe solubility experiments. Thus it is very likely that there is another size fraction of organic ligands between 100 kDa and 0.2 µm that was not monitored, but that could be captured in the future though the use of larger MWCO membranes (1000 kDa or larger). However, Fe solubilities measured for the fraction > 5 kDa are close to concentrations of dissolved organic Fe ligands determined in seawater by voltammetry (Boye et al. 2001; Croot et al. 2001; Powell and Donat 2001).

Fig. 3b shows the ratio of Fe solubility determined by the different MCWO Vivaspin membranes and Fe_D in the water column. This ratio appears useful to quantify the maximum capacity of seawater for soluble and colloidal organically complexed Fe. Conspicuously, all cFe_S/Fe_D ratios showed highest values near the surface (20 m), whereas significantly lower ratios were calculated for the subsurface samples. This implies that up to ten times more Fe in the colloidal size fraction between > 5 kDa and 10 kDa could be held in the near surface waters. In the "truly" soluble size fraction ≤ 5 kDa, twice as much Fe than present in the dissolved Fe pool could be held in these surface waters. This result has strong implications for the biogeochemical Fe cycle in this oceanic environment. The surface waters measured are not fully Fe saturated and may hold more Fe by organic complexation in the dissolved pool. Turbulent and diffusive mixing may be strong enough to transfer a reasonable quantity of Fe(II) and Fe(III) through the oxycline (~60 m) into the biological active oxygenated euphotic zone (Fig. 3). Regenerated Fe(III) formed below the mixed layer could be stabilized in the upper 70 m of the water column by the large amount of freely available organic chelators in the soluble and colloidal size fractions.

The ultrafiltration experiments performed here suggest that significantly more Fe in seawater can be held in the fraction between > 5–10 kDa than in the "truly" soluble fraction ≤ 5 kDa. This implies that ultrafiltration membranes ≥ 10 kDa are insufficient for separating the "truly" soluble from the colloidal fraction of organically complexed Fe. Consequently, Fe solubility determinations using 0.02 µm Anotop syringe filtration or 5 kDa membrane filtration experiments probably strongly underestimate the amount of organic chelators produced by remineralization (Schlosser and Croot 2009). These findings have strong implications for Fe models using the linear relationship between 0.02 µm Fe solubility and phosphate as key parameters for the production of organic chelators (Ye et al. 2009) by remineralization processes.

Fe solubility's and CDOM content

Investigations of Fe solubility and CDOM abundance during several expeditions in the Pacific Ocean showed a strong linear relationship between these two parameters (Tani et al. 2003; Kitayama et al. 2009; Yamashita et al. 2010). This relationship was attributed to the microbial decomposition of organic matter and the simultaneous release of humic-like substances and organic Fe chelators (Chen et al. 2004). It was also discussed that humic-like substances have several functional groups that could act directly as Fe chelators (Kuma and Isoda 2003; Tani et al. 2003; Chen et al. 2004; Kitayama et al. 2009; Laglera and Van Den Berg 2009).

Emission-excitation matrixes (EEM) were generated to identify different fluorescent substances via PARAFAC modeling (Table S1). Using the EEM-PARAFAC approach, two humic compounds (humic1 and humic2, Yamashita et al. 2010) and one protein compound were found in the samples in this study (Table 2). Humic compounds identified by PARAFAC and by the discrete single excitation-emission humic fluorescence data showed a weak but significant linear relationship

Table S1. Results for dissolved Fe (Fe_D), Fe solubility (0.02 μm Anotop syringe filtration), $CDOM_{320/420}$ fluorescence in Raman units for all other stations during M77-3 (white stars in Fig. 2). In addition, Humic1, Humic2, and Protein1 in Raman units computed by the PARAFAC algorithm using the entire EEM dataset of samples collected during M77-3.

Station	Latitude (°S)	Longitude (°W)	Depth (m)	Fe_D (nmol L^{-1})	cFe_S (nmol L^{-1})	$CDOM_{320/420}$ (R.U.)	Humic1 (R.U.)	Humic2 (R.U.)	Protein (R.U.)
1	10	78.38	20	3.46	0.57	0.114	0.016	0.016	0.035
30/12/08			40	1.77	0.37	0.083	0.013	0.011	0.027
08:04			60	10.91	0.42	0.062	0.009	0.007	0.021
3	10	78.38	5	2.72	0.58	0.084	0.016	0.013	0.021
30/12/08			40	2.02	0.69	0.112	0.018	0.017	0.021
20:03			60	4.55	0.55	0.082	0.014	0.013	0.018
			80	13.07	0.74	0.122	0.020	0.018	0.026
4	10	78.38	5	6.36	0.67	0.114	0.021	0.017	0.033
30/12/08			40	2.17	0.43	0.056	0.010	0.008	0.032
23:45			60	2.45	0.71	0.108	0.018	0.016	0.023
			80	18.93		0.034	0.008	0.006	0.023
6-7	10	79.47	20	0.56	0.30	0.046	0.008	0.011	0.058
01/01/09			75	0.43	0.41	0.063	0.009	0.012	0.054
13:40			140	0.34	0.37	0.049	0.007	0.009	0.048
			190	1.06	0.64	0.088	0.014	0.014	0.050
			300	1.31	0.47	0.068	0.012	0.009	0.029
			400	0.98	0.43	0.061	0.011	0.008	0.031
			600	1.84	0.40	0.074	0.012	0.010	0.034
			800	1.97	0.32	0.070	0.012	0.008	0.025
8-9	10	84	40	0.48	0.24	0.062	0.008	0.009	0.023
04/01/09			110	0.68	0.77	0.137	0.018	0.017	0.020
13:00			150	0.86	0.54	0.139	0.020	0.015	0.018
			200	1.27	0.81	0.124	0.019	0.015	0.021
			300	1.00	0.34	0.096	0.015	0.012	0.037
			400	0.43	0.52	0.130	0.021	0.015	0.029
			600	1.15	0.54	0.123	0.021	0.013	0.031
			800	1.50	0.36	0.101	0.013	0.012	0.025
12	12.03	78	10	2.88	0.46	0.136	0.020	0.021	0.048
08/01/09			75	4.15	0.63	0.139	0.011	0.013	0.028
00:55			150	6.45	0.43	0.077	0.020	0.015	0.016
			200	0.84		0.102			
18	18	73.42	25	0.81	0.51	0.065	0.009	0.012	0.027
17/01/09			50	0.98	0.37	0.091	0.012	0.012	0.023
15:16			100	2.78	0.60	0.140	0.018	0.017	0.021
			200	2.79	0.55	0.113	0.016	0.013	0.020

with Fe solubility determined using the 0.02 μm syringe filter and the 5 kDa membrane (Fig. 4a, 4b, 4c). This was not true with Fe solubility results from the 10 kDa membrane or even larger MWCO ultrafiltration membranes (Fig. 4a), with the resulting correlation being not statistically significant.

At present there is insufficient data to deduce if colloidal organic chelators are formed by the same processes as humic substances, or if humic substances in the colloidal size fraction are able to complex Fe. Future work needs to examine these aspects of iron biogeochemistry in seawater in more detail to elucidate more fully the role of remineralization in the generation of iron binding ligands and its influence on iron solubility.

Comments and recommendations

Vivaspin6 ultrafiltration devices for trace metal and trace metal speciation analysis are faster and probably also more reliable than conventional ultrafiltration devices, such as Vivaflow 50 cartridges or 0.02 μm Anotop syringe filters. By
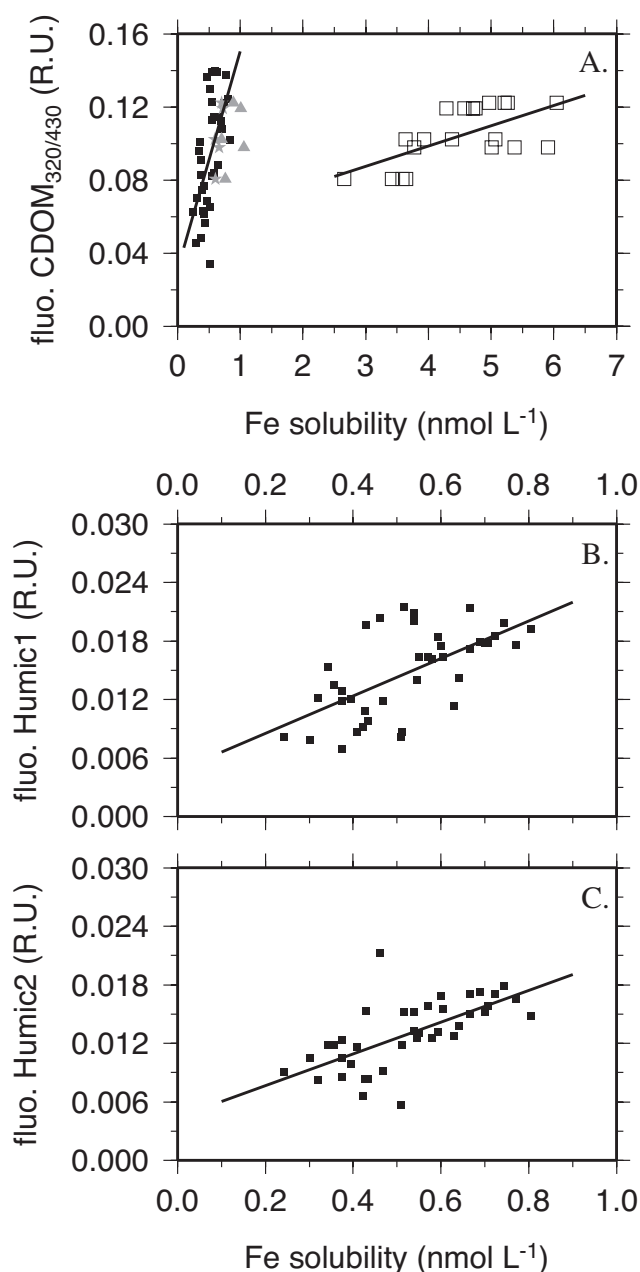
Fig. 4. (A) Linear regressions of Fe solubility and $CDOM_{320/420}$ fluorescence in Raman units. Black squares correspond to Fe solubility determined using 0.02 μm Anotop syringe filtration (Table S1). The remaining symbols refer to results from GoFlo station 10-11. Gray stars indicate Fe solubility determined using 0.02 μm Anotop syringe filtration. Fe solubility determined using 5 kDa membrane are illustrated by gray triangles, whereas cFe_S determined using 10, 30, 50, and 100 kDa membranes are shown by open squares. The linear regression for Anotop syringe filtration samples ($CDOM_{320/420} = 0.122 \times cFe_S + 0.03$, $R^2 = 0.46$ [Student t test, t($P = 0.001$) = 3.551 < 3.702]) has a different slope than for the ≥ 10 kDa ultrafiltration membranes ($CDOM_{320/420} = 0.011 \times cFe_S + 0.054$, $R^2 = 0.41$ [Student t test, t($P = 0.8$) = 0.256 > 0.019]). (B and C) Show the linear correlation of Fe solubility determined by 0.02 μm Anotop syringe filtration with the concentration of humic substances (fluo. humic1 [$Humic1 = 0.020 \times cFe_S + 0.05$, $R^2 = 0.46$] and fluo. humic2 [$Humic2 = 0.016 \times cFe_S + 0.04$, $R^2 = 0.61$]) that were identified by the PARAFAC algorithm.

using one of these devices equipped with a 5kDa MWCO polyethersulfone membrane, the "truly" soluble and colloidal fractions of trace metals and their complexing agents in natural seawater samples can be separated and analyzed. For example, the growth of inorganic Fe colloids could be investigated in Fe solubility incubations by monitoring several successive subsamples instead of just the one at the end of the incubation. Later on, combined with natural or artificial organic chelators, these experiments could help us to understand the processes of natural dust dissolution, particle formation, and Fe removal. The relatively small sample volume that can be passed through the Vivaspin6 ultrafiltration membrane represents the largest disadvantage of this method (5–6 times the reservoir volume; or ~ 36 mL for the Vivaspin 6; personal communication with Sartorius). When larger volumes must be processed, we recommend the Vivaspin15, Vivaspin20, or the conventional Vivaflow50 device. We are certain that brief temperature changes during sample centrifugation did not influence the Fe solubility equilibrium established after several days. However, if larger sample volumes are to be filtered for long periods of time we recommend using a temperature-controlled centrifuge to prevent possible treatment artifacts. As ultrafiltration is a commonly used technique with the potential to become a frequently used procedure in the current GEOTRACES sampling program, "intercalibration" measurements using ultrafiltration membranes (PES, polyacrylic, etc.) and devices (Vivaspin, Vivaflow, hollow fiber filters, etc.) are urgently needed to eliminate possible analytical artifacts from the collective results.

References

Achterberg, E. P., C. B. Braungardt, R. C. Sandford, and P. J. Worsfold. 2001. UV digestion of seawater samples prior to the determination of copper using flow injection with chemiluminescence detection. Anal. Chim. Acta 440:27-36 [doi:10.1016/S0003-2670(01)00824-8].

Barbeau, K., E. L. Rue, C. G. Trick, K. W. Bruland, and A. Butler. 2003. Photochemical reactivity of siderophores produced by marine heterotrophic bacteria and cyanobacteria based on characteristic Fe(III) binding groups. Limnol. Oceanogr. 48:1069-1078 [doi:10.4319/lo.2003.48.3.1069].

Batinic-Haberle, I., I. Spasojevic, and A. L. Crumbliss. 1994. Hydrolysis of Ferrioxamine B in aqueous micellar solution. Inorg. Chem. 33:3151-3158 [doi:10.1021/ic00092a022].

Boye, M., C. M. G. Van Den Berg, J. T. M. De Jong, H. Leach, P. L. Croot, and H. J. W. De Baar. 2001. Organic complexation of iron in the Southern Ocean. Deep-Sea Res. I 48:1477-1497 [doi:10.1016/S0967-0637(00)00099-6].

———, J. Nishioka, P. Croot, P. Laan, K. R. Timmermans, V. H. Strass, S. Takeda, and H. J. W. De Baar. 2010. Significant portion of dissolved organic Fe complexes in fact is Fe colloids. Mar. Chem. 122:20-27 [doi:10.1016/j.marchem.2010.09.001].

Bruland, K. W., R. P. Franks, G. A. Knauer, and J. H. Martin.

1979. Sampling and analytical methods for the determination of copper, cadmium, zinc, and nickel at the nanogram per liter level in sea water. Anal. Chim. Acta 105:233-245 [doi:10.1016/S0003-2670(01)83754-5].

Cheah, S.-F., S. M. Kraemer, J. Cervini-Silva, and G. Sposito. 2003. Steady-state dissolution kinetics of goethite in the presence of desferrioxamine B and oxalate ligands: implications for the microbial acquisition of iron. Chem. Geol. 198:63-75 [doi:10.1016/S0009-2541(02)00421-7].

———, ———, ———and ———. 2006. Erratum to "Steady-state dissolution kinetics of goethite in the presence of desferrioxamine B and oxalate ligands: Implications for the microbial acquisition of iron" [Chemical Geology 198 (2003) 63–75]. Chem. Geol. 228:290 [doi:10.1016/j.chemgeo.2005.11.002].

Chen, M., W.-X. Wang, and L. Guo. 2004. Phase partitioning and solubility of iron in natural seawater controlled by dissolved organic matter. Global Biogeochem. Cycles 18:1-12 [doi:10.1029/2003GB002160].

Croot, P. L., and M. Johansson. 2000. Determination of iron speciation by cathodic stripping voltammetry in seawater using the competing ligand 2-(2-Thiazolylazo)-p-cresol (TAC). Electroanalysis 12:565-576 [doi:10.1002/(SICI)1521-4109(200005)12:8<565::AID-ELAN565>3.0.CO;2-L].

———, and others. 2001. Retention of dissolved iron and Fe II in an iron induced Southern Ocean phytoplankton bloom. Geophys. Res. Lett. 28:3425-3428 [doi:10.1029/2001GL013023].

———, B. Karlson, J. T. Van Elteren, and J. J. Kroon. 2003. Uptake and efflux of 64Cu by the marine cyanobacterium Synechococcus (WH7803). Limnol. Oceanogr. 48:179-188 [doi:10.4319/lo.2003.48.1.0179].

———, K. Andersson, M. Öztürk, and D. Turner. 2004a. The distribution and speciation of iron along 6° E, in the Southern Ocean. Deep-Sea Res. II 51:2857-2879 [doi:10.1016/j.dsr2.2003.10.012].

———, P. Streu, and A. R. Baker. 2004b. Short residence time for iron in surface seawater impacted by atmospheric dry deposition from Saharan dust events. Geophys. Res. Lett. 31:1-4 [doi:10.1029/2004GL020153].

———, M. I. Heller, C. Schlosser, and K. Wuttig. 2011. Utilizing radioisotopes for trace metal measurements in seawater. *In* N. Singh [ed.], Radioisotopes—Applications in physical Sciences. InTech.

Danielsson, L.-G., B. Magnusson, and S. Westerlund. 1978. An improved metal extraction procedure for the determination of trace metals in sea water by atomic absorption spectrometry with electrothermal atomization. Anal. Chim. Acta 98:47-57 [doi:10.1016/S0003-2670(01)83237-2].

Essington, M. E., J. B. Nelson, and W. L. Holden. 2005. Gibbsite and goethite solubility: The influence of 2-ketogluconate and citrate. Soil Sci. Soc. Am. J. 69:996-1008 [doi:10.2136/sssaj2004.0287].

Gerringa, L. J. A., H. J. W. De Baar, and K. R. Timmermans. 2000. A comparison of iron limitation of phytoplankton in natural oceanic waters and laboratory media conditioned with EDTA. Mar. Chem. 53:255-267.

Gobler, C. J., D. A. Hutchins, N. S. Fisher, E. M. Cosper, and S. A. Sanudo-Wilhelmy. 1997. Release and bioavailability of C, N, P, Se, and Fe following viral lysis of a marine chrysophyte. Limnol. Oceanogr. 42:1492-1504 [doi:10.4319/lo.1997.42.7.1492].

Grasshoff, K., M. Erhardt, and K. Kremling. 1999. Methods of seawater analysis, 3 ed. Wiley-VCH.

Guo, L., B. J. Hunt, and P. H. Santschi. 2001. Ultrafiltration behavior of major ions (Na, Ca, Mg, F, Cl, AND SO4) in natural waters. Water Res. 35:1500-1508 [doi:10.1016/S0043-1354(00)00407-3].

Hassellöv, M., K. O. Buesseler, S. M. Pike, and M. Dai. 2007. Application of cross-flow ultrafiltration for the determination of colloidal abudances in suboxic ferrous-rich ground waters. Sci. Total Environ. 372:636-644 [doi:10.1016/j.scitotenv.2006.10.001].

Hong, H., and D. R. Kester. 1986. Redox state of iron in the offshore waters of Peru. Limnol. Oceanogr. 31:512-524 [doi:10.4319/lo.1986.31.3.0512].

Hove, M., R. P. Van Hille, and A. E. Lewis. 2007. Iron solids formed from oxidation precipitation of ferrous sulfate solutions. AlChE J. 53:2569-2577 [doi:10.1002/aic.11264].

Hovind, H. R. 1975. Thiazolylazo dyes and their applications in analytical chemistry. Analyst 100:769-796 [doi:10.1039/an9750000769].

Hudson, R. J. M., D. T. Covault, and F. M. M. Morel. 1992. Investigations of iron coordination and redox reactions in seawater using 59Fe radiometry and ion-pair solvent extraction of amphiphilic iron complexes. Mar. Chem. 38:209-235 [doi:10.1016/0304-4203(92)90035-9].

Hutchins, D. A., V. M. Franck, M. A. Brzezinski, and K. W. Bruland. 1999. Inducing phytoplankton iron limitation in iron-replete coastal waters with a strong chelating ligand. Limnol. Oceanogr. 44:1009-1018 [doi:10.4319/lo.1999.44.4.1009].

Iwade, S., K. Kuma, Y. Isoda, M. Yoshida, I. Kudo, J. Nishioka, and K. Suzuki. 2006. Effect of high iron concentrations on iron uptake and growth of a coastal diatom Chaetoceros sociale. Aquat. Microb. Ecol. 43:177-191 [doi:10.3354/ame043177].

Kim, D., O. W. Duckworth, and T. J. Strathmann. 2010. Reactions of aqueous iron-DFOB (desferrioxamine B) complexes with flavin mononucleotide in the absence of strong iron(II) chelators. Geochim. Cosmochim. Acta 74:1513-1529 [doi:10.1016/j.gca.2009.12.020].

Kitayama, S., and others. 2009. Controls on iron distributions in the deep water column of the North Pacific Ocean: Iron(III) hydroxide solubility and marine humic-type dissolved organic matter. J. Geophys. Res. 114:1-13 [doi:10.1029/2008JC004754].

Kuma, K., and K. Matsunaga. 1995. Availability of colloidal

ferric oxides to coastal marine phytoplankton. Mar. Biol. 122:1-11 [doi:10.1007/BF00349272].

———, J. Nishioka, and K. Matsunaga. 1996. Controls on iron(III) hydroxide solubility in seawater: The influence of pH and natural organic chelators. Limnol. Oceanogr. 41:396-407 [doi:10.4319/lo.1996.41.3.0396].

———, and Y. Isoda. 2003. Control on dissolved iron concentrations in deep waters in the western North Pacific: Iron(III) hydroxide solubility. J. Geophys. Res. 108:1-10 [doi:10.1029/2002JC001481].

Laglera, L. M., and C. M. G. Van Den Berg. 2009. Evidence for geochemical control of iron by humic substances in seawater. Limnol. Oceanogr. 54:610-619 [doi:10.4319/lo.2009.54.2.0610].

Lawaetz, A. J., and C. A. Stedmon. 2009. fluorescence intensity calibration using the raman scatter peak of water. Appl. Spectrosc. 63:936-940 [doi:10.1366/000370209788964548].

Liu, H., and F. J. Millero. 1999. The solubility of iron hydroxide in sodium chloride solutions. Geochim. Cosmochim. Acta 63:3487-3497 [doi:10.1016/S0016-7037(99)00270-7].

———, and F. J. Millero. 2002. The solubility of iron in seawater. Mar. Chem. 77:43-54 [doi:10.1016/S0304-4203(01)00074-3].

Lohan, M. C., and K. W. Bruland. 2008. Elevated Fe(II) and dissolved fe in hypoxic shelf waters off Oregon and Washington: An enhanced source of iron to coastal upwelling regimes. Environ. Sci. Technol. 42:6462-6468 [doi:10.1021/es800144j].

Martinez, J. S., G. P. Zhang, P. D. Holt, H.-T. Jung, C. J. Carrano, M. G. Haygood, and A. Butler. 2000. Self-assembling amphiphilic siderophores from marine bacteria. Science 287:1245-1247 [doi:10.1126/science.287.5456.1245].

Mopper, K., and C. A. Schultz. 1993. Fluorescence as a possible tool for studying the nature and water column distribution of DOC components. Mar. Chem. 41:229-238 [doi:10.1016/0304-4203(93)90124-7].

Nakabayashi, S., K. Kuma, K. Sasaoka, S. Saitoh, M. Mochizuki, N. Shiga, and M. Kusakabe. 2002. Variation in iron(III) solubility and iron concentration in the northwestern North Pacific Ocean. Limnol. Oceanogr. 47:885-892 [doi:10.4319/lo.2002.47.3.0885].

Ndung'u, K., R. P. Franks, K. W. Bruland, and A. R. Flegal. 2003. Organic complexation and total dissolved trace metal analysis in estuarine waters: comparison of solvent-extraction graphite furnace atomic absorption spectrometric and chelating resin flow injection inductively coupled plasma-mass spectrometric analysis. Anal. Chim. Acta 481:127-138 [doi:10.1016/S0003-2670(03)00063-1].

Nelson, J. B., and M. E. Essington. 2005. The association constants of H+ and Ca2+ with 2-keto-D-gluconate in aqueous solutions. J. Solution Chem. 34:789-800 [doi:10.1007/s10953-005-5116-7].

Nishioka, J., S. Takeda, C. S. Wong, and W. K. Johnson. 2001. Size-fractionated iron concentrations in the northeast Pacific Ocean: distribution of soluble and small colloidal iron. Mar. Chem. 74:157-179 [doi:10.1016/S0304-4203(01)00013-5].

Nowostawska, U., J. P. Kim, and K. A. Hunter. 2008. Aggregation of riverine colloidal iron in estuaries: A new kinetic study using stopped-flow mixing. Mar. Chem. 110:205-210 [doi:10.1016/j.marchem.2008.03.001].

Owen, T., and A. Butler. 2011. Metallosurfactants of bioinorganic interest: Coordination-induced self assembly. Coord. Chem. Rev. 255:678-687 [doi:10.1016/j.ccr.2010.12.009].

Öztürk, M., P. L. Croot, S. Bertilsson, K. Abrahamsson, B. Karlson, R. David, A. Fransson, and E. Sakshaug. 2004. Iron enrichment and photoreduction of iron under PAR and UV in the presence of hydrocarboxylic acid: Implications for phytoplankton growth in the Southern Ocean. Deep-Sea Res. II 51:2841-2856 [doi:10.1016/j.dsr2.2000.10.001].

Powell, R. T., and J. R. Donat. 2001. Organic complexation and speciation of iron in the South and Equatorial Atlantic. Deep-Sea Res. II 48:2877-2893 [doi:10.1016/S0967-0645(01)00022-4].

Reitmeyer, R., R. T. Powell, W. M. Landing, and C. I. Measures. 1996. Colloidal aluminum and iron in seawater: An intercomparison between various cross-flow ultrafiltration systems. Mar. Chem. 55:75-91 [doi:10.1016/S0304-4203(96)00049-7].

Rue, E. L., and K. W. Bruland. 1995. Complexation of iron(III) by natural organic-ligands in the Central North Pacific as determined by a new competitive ligand equilibration adsorptive cathodic stripping voltammetric method. Mar. Chem. 50:117-138 [doi:10.1016/0304-4203(95)00031-L].

———, and ———. 1997. The role of organic complexation on ambient iron chemistry in the equatorial Pacific Ocean and the response of a mesoscale iron addition experiment. Limnol. Oceanogr. 42:901-910 [doi:10.4319/lo.1997.42.5.0901].

Sato, M., S. Takeda, and K. Furuya. 2007. Iron regeneration and organic iron(III)-binding ligand production during in situ zooplankton grazing experiment. Mar. Chem. 106:471-488 [doi:10.1016/j.marchem.2007.05.001].

Schlosser, C., and P. L. Croot. 2008. Application of cross-flow filtration for determining the solubility of iron species in open ocean seawater. Limnol. Oceanogr. Methods 6:630-642 [doi:10.4319/lom.2008.6.630].

———, and ———. 2009. Controls on seawater Fe(III) solubility in the Mauritanian upwelling zone. Geophys. Res. Lett. 36:1-5.

———, C. L. De La Rocha, and P. L. Croot. 2011. Effects of iron surface adsorption and sample handling on iron solubility measurements. Mar. Chem. 127:48-55 [doi:10.1016/j.marchem.2011.07.008].

Schwarzenbach, G., and K. Schwarzenbach. 1963. Hydroxamatkomplexe I. Die Stabilitat der Eisen(III)-Komplexe einfacher Hydroxamsauren und des Ferrioxamins B. Helv. Chim. Acta 46:1390-1401 [doi:10.1002/hlca.19630460434].

Stedmon, C. A., S. Markager, and R. Bro. 2003. Tracing dissolved organic matter in aquatic environments using a new approach to fluorescence spectroscopy. Mar. Chem. 82:239-254 [doi:10.1016/S0304-4203(03)00072-0].

———, and R. Bro. 2008. Characterizing dissolved organic matter fluorescence with parallel factor analysis: a tutorial. Limnol. Oceanogr. Methods 6:572-579 [doi:10.4319/lom.2008.6.572].

Stolpe, B., and M. Hassellov. 2010. Nanofibrils and other colloidal biopolymers binding trace elements in coastal seawater: Significance for variations in element size distributions. Limnol. Oceanogr. 55:187-202 [doi:10.4319/lo.2010.55.1.0187].

Sunda, W., and S. Huntsman. 2003. Effect of pH, light, and temperature on Fe–EDTA chelation and Fe hydrolysis in seawater. Mar. Chem. 84:35-47 [doi:10.1016/S0304-4203(03)00101-4].

Tani, H., J. Nishioka, K. Kuma, H. Takata, Y. Yamashita, E. Tanoue, and T. Midorikawa. 2003. Iron(III) hydroxide solubility and humic-type fluorescent organic matter in the deep water column of the Okhotsk Sea and the northwestern North Pacific Ocean. Deep-Sea Res. I 50:1063-1078 [doi:10.1016/S0967-0637(03)00098-0].

Waite, T. D., A. I. Schäfer, A. G. Fane, and A. Heuer. 1999. Colloidal fouling of ultrafiltration membranes: impact of aggregate structure and size. J. Colloid. Interf. Sci. 212:264-274 [doi:10.1006/jcis.1998.6040].

Witter, A. E., and G. W. Luther. 1998. Variation in Fe-organic complexation with depth in the Northwestern Atlantic Ocean as determined using a kinetic approach. Mar. Chem. 62:241-258 [doi:10.1016/S0304-4203(98)00044-9].

Wu, J., E. Boyle, W. Sunda, and L. Wen. 2001. Soluble and colloidal iron in the oligotrophic North Atlantic and North Pacific. Science 293:847-849 [doi:10.1126/science.1059251].

Yamashita, Y., R. M. Cory, J. Nishioka, K. Kuma, E. Tanoue, and R. Jaffé. 2010. Fluorescence characteristics of dissolved organic matter in the deep waters of the Okhotsk Sea and the northwestern North Pacific Ocean. Deep-Sea Res. II 57:1478-1485 [doi:10.1016/j.dsr2.2010.02.016].

Ye, Y., C. Völker, and D. A. Wolf-Gladrow. 2009. A model of Fe speciation and biogeochemistry at the Tropical Eastern North Atlantic Time-Series Observatory site. Biogeosciences 6:2041-2061 [doi:10.5194/bg-6-2041-2009].

Yoshida, M., K. Kuma, S. Iwade, Y. Isoda, H. Takata, and M. Yamada. 2006. Effect of aging time on the availability of freshly precipitated ferric hydroxide to costal marine diatoms. Mar. Biol. 149:379-392 [doi:10.1007/s00227-005-0187-y].

Queries
Q1. Please provide 40 characters and spaces or less.
Q2. Per journal style, please include first names.
Q3. Hayase et al. (1988) not in references. Please add.
Q4. Hayase and Shinozuka (1995) not in references. Please add.
Q5. Changed date per journal style. Are date and month correct?